

1 **Risk factors affecting polygenic score performance across diverse cohorts**

2 Daniel Hui¹, Scott Dudek¹, Krzysztof Kiryluk², Theresa L. Walunas³, Iftikhar J. Kullo⁴, Wei-Qi
3 Wei⁵, Hemant K. Tiwari⁶, Josh F. Peterson⁵, Wendy K. Chung⁷, Brittney Davis⁸, Atlas Khan²,
4 Leah Kottyan⁹, Nita A. Limdi⁸, Qiping Feng¹⁰, Megan J. Puckelwartz¹¹, Chunhua Weng¹²,
5 Johanna L. Smith⁴, Elizabeth W. Karlson¹³, Regeneron Genetics Center¹⁴, Gail P. Jarvik¹⁵,
6 Marylyn D. Ritchie¹

7
8 ¹Department of Genetics, Perelman School of Medicine, University of Pennsylvania,
9 Philadelphia, PA.

10 ²Division of Nephrology, Department of Medicine, Columbia University, NY, New York.

11 ³Department of Preventive Medicine, Northwestern University Feinberg School of Medicine,
12 Chicago, Illinois, USA.

13 ⁴Department of Cardiovascular Medicine, Mayo Clinic, Rochester, MN.

14 ⁵Department of Biomedical Informatics, Vanderbilt University Medical Center, Nashville, TN.

15 ⁶Department of Pediatrics, University of Alabama at Birmingham, Birmingham, AL.

16 ⁷Departments of Pediatrics and Medicine, Columbia University Irving Medical Center, Columbia
17 University, New York, NY.

18 ⁸Department of Neurology, School of Medicine, University of Alabama at Birmingham,
19 Birmingham, AL.

20 ⁹The Center for Autoimmune Genomics and Etiology, Division of Human Genetics, Cincinnati
21 Children's Hospital Medical Center, Cincinnati, OH.

22 ¹⁰Division of Clinical Pharmacology, Department of Medicine, Vanderbilt University Medical
23 Center, Nashville, TN, USA.

24 ¹¹Center for Genetic Medicine, Northwestern University Feinberg School of Medicine, Chicago,
25 IL.

26 ¹²Department of Biomedical Informatics, Vagelos College of Physicians & Surgeons, Columbia
27 University, New York, NY.

28 ¹³Division of Rheumatology, Inflammation, and Immunity, Department of Medicine, Brigham
29 and Women's Hospital and Harvard Medical School, Boston, MA.

30 ¹⁴Regeneron Pharmaceuticals Inc., Tarrytown, NY.

31 ¹⁵Departments of Medicine (Medical Genetics) and Genome Sciences, University of Washington
32 Medical Center, Seattle, WA.

33

34 Correspondence to:

35 Marylyn D. Ritchie, PhD

36 marylyn@pennmedicine.upenn.edu

37

38

39

40

41

42

43

44

45

46

47 **Abstract**

48 Apart from ancestry, personal or environmental covariates may contribute to differences in
49 polygenic score (PGS) performance. We analyzed effects of covariate stratification and
50 interaction on body mass index (BMI) PGS (PGS_{BMI}) across four cohorts of European
51 ($N=491,111$) and African ($N=21,612$) ancestry. Stratifying on binary covariates and quintiles for
52 continuous covariates, 18/62 covariates had significant and replicable R^2 differences among
53 strata. Covariates with the largest differences included age, sex, blood lipids, physical activity,
54 and alcohol consumption, with R^2 being nearly double between best and worst performing
55 quintiles for certain covariates. 28 covariates had significant PGS_{BMI} -covariate interaction
56 effects, modifying PGS_{BMI} effects by nearly 20% per standard deviation change. We observed
57 overlap between covariates that had significant R^2 differences among strata and interaction
58 effects – across all covariates, their main effects on BMI were correlated with their maximum R^2
59 differences and interaction effects (0.56 and 0.58, respectively), suggesting high- PGS_{BMI}
60 individuals have highest R^2 and increase in PGS effect. Using quantile regression, we show the
61 effect of PGS_{BMI} increases as BMI itself increases, and that these differences in effects are
62 directly related to differences in R^2 when stratifying by different covariates. Given significant
63 and replicable evidence for context-specific PGS_{BMI} performance and effects, we investigated
64 ways to increase model performance taking into account non-linear effects. Machine learning
65 models (neural networks) increased relative model R^2 (mean 23%) across datasets. Finally,
66 creating PGS_{BMI} directly from GxAge GWAS effects increased relative R^2 by 7.8%. These
67 results demonstrate that certain covariates, especially those most associated with BMI,
68 significantly affect both PGS_{BMI} performance and effects across diverse cohorts and ancestries,
69 and we provide avenues to improve model performance that consider these effects.

70
71
72
73
74
75
76
77
78
79
80
81
82
83
84
85
86
87
88
89
90
91
92

93 Introduction

94 Polygenic scores (PGS) provide individualized genetic predictors of a phenotype by aggregating
95 genetic effects across hundreds or thousands of loci, typically estimated from genome-wide
96 association studies (GWAS). In recent years it has become increasingly apparent that the
97 transferability of PGS performance across different cohorts is poor (1). Most analyses to date
98 have focused on ancestry differences as the main driver of this lack of portability (2–4).
99 However, a growing body of evidence has demonstrated that PGS performance and effect
100 estimates are influenced by differences in certain contexts i.e., environmental (classically termed
101 “gene-environment” effects or interactions) or personal-level covariates – different phenotypes
102 seem to be differently affected by these covariates, with adiposity traits such as body mass index
103 (BMI) having substantial evidence for these effects (5–14). In one previous study, they showed
104 that GWAS stratified by sample characteristics had better PGS performance in cohorts that
105 matched the sample characteristics of the stratified GWAS, and that differences in heritability
106 between the stratified cohorts partially explained this observation (13).

107 There are several gaps in current knowledge about these covariate-specific effects. Many
108 analyses have assessed only a handful of these covariates due to the myriad of choices possible
109 in typical large-scale biobanks. Little investigation has been done to systematically understand
110 why certain covariates affect PGS performance, with such knowledge being useful to reduce the
111 potential search for variables that impart context-specific effects. Furthermore, most studies
112 investigating PGS-covariate interactions have been in European ancestry individuals; notably,
113 comparing differences in PGS performance and prediction while controlling for differences in
114 ancestry versus differences in context has not been assessed in previous studies. Moreover,
115 covariate-specific effects are notorious for replicating poorly in human genetics studies, and
116 previous studies of PGS-covariate interactions have been predominantly performed in the UK
117 Biobank (UKBB) (15), where the majority of individuals are aged 40-69 (i.e., excluding young
118 adults), are overall healthier than those from other e.g., hospital-based cohorts, and are
119 predominantly European ancestry. Additionally, PGS performance is often assessed using linear
120 models and in isolation of clinical covariates, which in practice would often be available.
121 Machine learning models can have increased performance over linear models and are capable of
122 modeling complex relationships and interactions between variables, which may serve to increase
123 predictive performance, especially given evidence for PGS-covariate specific effects. Finally,
124 given evidence for context-specific effects, it should be possible to directly incorporate SNP-
125 covariate interaction effects from a GWAS directly to improve prediction performance, instead
126 of relying on post-hoc interactions from a typical PGS calculated from main GWAS effects.

127 Using genetic data with linked-phenotypic information from electronic health records, we
128 estimated the effects of covariate stratification and interaction on performance and effect
129 estimates of PGS for BMI (PGS_{BMI}) – a flowchart summarizing our analyses is presented in
130 Figure 1. These analyses were done across four datasets (Supplemental Table 1): UK Biobank
131 (UKBB), Penn Medicine BioBank (PMBB) (15), Electronic Medical Records and Genomics
132 (eMERGE) network dataset (16), and Genetic Epidemiology Research on Adult Health and
133 Aging (GERA). These datasets include participants from two ancestry groups (N=491,111
134 European ancestry (EUR), N=21,612 African ancestry (AFR)), and 62 covariates (25 present in
135 multiple datasets) representing laboratory, survey, and biometric data types typically associated
136 with cardiometabolic health and adiposity. After constructing PGS_{BMI} using out-of-sample multi-
137 ancestry BMI GWAS, we assessed effects of covariate stratification on $PGS_{BMI} R^2$, the
138 significance of PGS_{BMI} -covariate interaction terms and their increases to model R^2 over models

139 only using main effects, as well as correlation of main effect, interaction effect, and R^2
140 differences. We then assessed ways to increase model performance through using machine
141 learning models, and creating PGS_{BMI} using GxAge GWAS effects. This study addresses a
142 plethora of open issues considering performance and effects of PGS on individuals from diverse
143 backgrounds.

144

145 **Results**

146 Effect of covariate stratification on PGS_{BMI} performance

147 We assessed 62 covariates for PGS_{BMI} R^2 differences (25 present, or suitable proxies, in multiple
148 datasets (Supplemental Table 2) after stratifying on binary covariates and quintiles for
149 continuous covariates. With UKBB EUR as discovery ($N=376,729$), 18 covariates had
150 significant differences (Bonferroni $p<.05/62$) in R^2 among groups (Figure 2a), including age, sex,
151 alcohol consumption, different physical activity measurements, Townsend deprivation index,
152 different dietary measurements, lipids, blood pressure, and HbA1c, with 40 covariates having
153 suggestive ($p<.05$) evidence of R^2 differences. From an original PGS_{BMI} R^2 of 0.076, R^2
154 increased to 0.094-0.088 for those in the bottom physical activity, alcohol intake, and high-
155 density lipoprotein (HDL) cholesterol quintiles, and decreased to 0.067-0.049 for those in the top
156 quintile, respectively, comparable to differences observed between ancestries (1). We note that
157 the differences in R^2 due to alcohol intake and HDL were larger than those of any physical
158 activity phenotype, despite physical activity having one of the oldest and most replicable
159 evidence of interaction with genetic effects of BMI (17,18). Despite considerable published
160 evidence suggesting covariate-specific genetic effects between BMI and smoking behaviors
161 (6,8), we were only able to find suggestive evidence for R^2 differences when stratifying
162 individuals across several smoking phenotypes (minimum $p=0.016$, for smoking pack years). R^2
163 differences due to educational attainment were also only suggestive ($p=0.015$), with published
164 evidence on this association being conflicting (19–21).

165 We replicated these analyses in three additional large-scale cohorts of European and
166 African ancestry individuals (Figure 2b, Supplemental Table 3), as well as in African ancestry
167 UKBB individuals. Among covariates with significant performance differences in the discovery
168 analysis, we were able to replicate significant ($p<.05$) R^2 differences for age, HDL cholesterol,
169 alcohol intake frequency, physical activity, and HbA1c, despite much smaller sample sizes. We
170 again observed mostly insignificant differences across cohorts and ancestries when stratifying
171 due to different smoking phenotypes and educational attainment. For each covariate and ancestry
172 combination, we combined data across cohorts and conducted a linear regression weighted by
173 sample size, regressing R^2 values on covariate values across groupings. Slopes of the regressions
174 across cohorts had different signs between ancestries for the same covariate (triglyceride levels,
175 HbA1c, diastolic blood pressure, and sex), although larger sample sizes may be needed to
176 confirm these differences are statistically significant.

177 Several observations related to age-specific effects on PGS_{BMI} we considered noteworthy.
178 First, in the weighted linear regression of all R^2 values across ancestries, expected R^2 for African
179 ancestry individuals can become greater than that of European ancestry individuals among
180 individuals within bottom and top age quintiles observed in these data. For instance, the
181 predicted R^2 of 0.048 for 80 year-old European ancestry individuals would be lower than that of
182 African ancestry individuals aged 24.7 and lower, indicating that differences in covariates can
183 affect PGS_{BMI} performance more than differences due to ancestry. Second, we obtained these
184 results despite the average age of GWAS individuals being 57.8, which should increase PGS_{BMI}

185 R^2 for individuals closest to this age (13). This result suggests that PGS performance due to
186 decreased heritability with age cannot be fully reconciled using GWAS from individuals of
187 similar age being used to create PGS_{BMI} (as heritability is an upper bound on PGS performance).
188 Finally, we observed that PGS_{BMI} R^2 increases as age decreases, consistent with published
189 evidence suggesting that the heritability of BMI decreases with age (22,23).

190

191 PGS-covariate interaction effects

192 Next, we estimated difference in PGS effects due to interactions with covariates, by modeling
193 interaction terms between PGS_{BMI} and the covariate for each covariate in our list (described in
194 Methods). We implemented a correction for shared heritability between covariates of interest and
195 outcome (which can inflate test statistics (24)) to better measure the environmental component of
196 each covariate, and show that this correction successfully reduces significance of interaction
197 estimates (Supplemental Figure 1). Again, using UKBB EUR as the discovery cohort, we
198 observed 28 covariates with significant (Bonferroni $p < .05/62$) PGS-covariate interactions (Table
199 1), with 38 having suggestive ($p < .05$) evidence (Supplemental Table 4). We observed the largest
200 effect of PGS-covariate interaction with alcohol drinking frequency (20.0% decrease in PGS
201 effect per 1 standard deviation (SD) increase, $p = 2.62 \times 10^{-55}$), with large effects for different
202 physical activity measures (9.4%-12.5% decrease/SD, minimum $p = 3.11 \times 10^{-66}$), HDL cholesterol
203 (15.3% decrease/SD, $p = 1.71 \times 10^{-96}$) and total cholesterol (12.7% decrease/SD, $p = 1.64 \times 10^{-71}$). We
204 observed significant interactions with diastolic blood pressure (10.8% increase/SD, $p = 6.06 \times 10^{-60}$),
205 but interactions with systolic blood pressure were much smaller (1.17% increase/SD,
206 $p = 4.41 \times 10^{-3}$). Significant interactions with HbA1c (4.63% increase/SD, $p = 5.37 \times 10^{-14}$) and type 2
207 diabetes (27.2% PGS effect increase in cases, $p = 1.83 \times 10^{-7}$) were also observed. Other significant
208 PGS-covariate interactions included lung function, age, sex, and LDL cholesterol – various
209 dietary measurements also had significant interactions, albeit with smaller effects than other
210 significant covariates. We were able to find significant interaction effects for smoking pack years
211 (4.78% increase/SD, $p = 3.68 \times 10^{-7}$), but other smoking phenotypes had insignificant interaction
212 effects after correcting for multiple tests (minimum $p = 2.7 \times 10^{-3}$); interactions with educational
213 attainment were also insignificant ($p = 4.54 \times 10^{-2}$).

214 We replicated these analyses across ancestries and the other non-UKBB EUR cohorts
215 (Figure 3, Supplemental Table 4). For age and sex, which were available for all cohorts,
216 interactions were significant ($p < .05$) and directionally consistent across cohorts and ancestries
217 (except for GERA AFR which had small sample size ($N = 1,789$)). We were able to test
218 interactions with alcohol intake frequency and physical activity in GERA, and replicated
219 significant and directionally consistent associations. We observed poor replication for LDL
220 cholesterol, HbA1c, and smoking pack years, with insignificant and directionally inconsistent
221 interaction effects across cohorts. Educational attainment was available in GERA, and
222 interactions were once again insignificant. We observed significant and directionally consistent
223 interaction effects for TG in eMERGE EUR and PMBB EUR, while the effect was inconsistent
224 in UKBB EUR despite much larger sample size.

225 However, despite significance of interaction terms, increases in model R^2 when including
226 PGS-covariate interaction terms were small. For instance, the maximum increase among all
227 covariates in UKBB EUR was only 0.0024 from a base R^2 of 0.1049 (2.1% relative increase), for
228 alcoholic drinks per week. Across all cohorts and ancestries, the maximum increase in R^2 was
229 only 0.0058 from a base R^2 of 0.09454 (6.1% relative increase), when adding a PGS-age
230 interaction term for eMERGE EUR ($p = 5.40 \times 10^{-46}$) – this was also the largest relative increase

231 among models with significant interaction terms. This result suggests that, while interaction
232 effects can significantly modify PGS_{BMI} effect, their overall impact on model performance is
233 relatively small, despite large differences in R^2 when stratifying by covariates.

234 235 Correlations between R^2 differences, interaction effects, and main effects

236 We next investigated the relationship between interaction effects, maximum R^2 differences
237 across quintiles, and main effects of covariates on BMI. We first estimated main effects of each
238 covariate on BMI (Methods, Supplemental Table 5), and then calculated the correlation weighted
239 by sample size between main effects, maximum PGS_{BMI} R^2 across quintiles, and PGS-covariate
240 interaction effects (Figure 4) across all cohorts and ancestries – GERA data were excluded from
241 these analyses due to slightly different phenotype definition (Supplemental Table 6), as were
242 binary variables. Interaction effects and maximum R^2 differences had a 0.80 correlation
243 ($p=2.1 \times 10^{-27}$), indicating that variables with larger interaction effects also had larger effects on
244 PGS_{BMI} performance across quintiles, and that covariates that increase PGS_{BMI} effect also have
245 the largest effect on PGS_{BMI} performance i.e., individuals most at risk for obesity will have both
246 disproportionately larger PGS_{BMI} effect and R^2 . Main effects and maximum R^2 differences had a
247 0.56 correlation ($p=1.3 \times 10^{-11}$), while main effects and interaction effects had a 0.58 correlation
248 ($p=7.6 \times 10^{-12}$) again suggesting that PGS_{BMI} are more predictive in individuals with higher values
249 of BMI-associated covariates, although less predictive than estimating the interaction effects
250 themselves directly. However, this result demonstrates that covariates that influence both PGS_{BMI}
251 effect and performance can be predicted just using main effects of covariates, which are often
252 known for certain phenotypes and easier to calculate, as genetic data and PGS construction
253 would not be required.

254 255 Increase in PGS effect for increasing percentiles of BMI itself, and its relation to R^2 differences 256 when stratifying by covariates

257 Given large and replicable correlations between main effects, interaction effects, and maximum
258 R^2 differences for individual covariates, it seemed these differences may be due to the
259 differences in BMI itself, rather than any individual or combination of covariates. To assess this,
260 we used quantile regression to evaluate the effect of PGS_{BMI} on BMI at different deciles of BMI
261 itself. We observed that the effect of PGS_{BMI} consistently increases from lower deciles to higher
262 deciles across all cohorts and ancestries (Figure 5) – for instance, in European ancestry UKBB
263 individuals, the effect of PGS_{BMI} (in units of $\log(\text{BMI})$) when predicting the bottom decile of
264 $\log(\text{BMI})$ was 0.716 (95% CI: 0.701-.732), and increased to 1.31 (95% CI: 1.29-1.33) in the top
265 decile. Across all cohorts and ancestries, the effect of PGS_{BMI} between lowest and highest effect
266 decile ranged from 1.43-2.06 times larger, with all cohorts and ancestries having non-
267 overlapping 95% confidence intervals between their effects (except for African ancestry
268 eMERGE individuals, which had much smaller sample size).

269 While this analysis showed that the effect of PGS_{BMI} increases as BMI itself increases,
270 which may help explain significant interaction effects between PGS_{BMI} and different covariates,
271 it does not directly explain differences in R^2 when stratifying by different covariates – we
272 describe several points that help explain this result and suggest they may actually be closely
273 related. Essentially, as the magnitude of the slope of a regression line increases while the mean
274 squared residual does not increase, model R^2 will increase – we demonstrate this using simulated
275 data (Supplemental Figure 2). As the magnitude of the regression line's slope decreases, the
276 regression line becomes a comparatively worse predictor compared to just using the mean, which

277 decreases R^2 despite the mean error being the same across models. To demonstrate this in real
278 data, we compared simple univariable models of $\log(\text{BMI}) \sim \text{PGS}_{\text{BMI}}$ (in units of $\log(\text{BMI})$)
279 between the bottom and top age quintiles in the European ancestry UKBB (Supplemental Figure
280 3). As shown in previous sections, R^2 and PGS_{BMI} beta are higher in younger individuals ($R^2 =$
281 0.088 versus $R^2 = 0.066$, and $\text{beta}=1.12$ and 0.87 , respectively), which seem to be a direct
282 consequence of one another, as the mean squared error in younger individuals is actually higher
283 (0.027 versus 0.022 , respectively). This description suggests that the use of R^2 as the sole
284 performance metric for evaluation of PGS may not always be appropriate, despite its
285 overwhelming usage. Furthermore, this explanation helps explain the seemingly paradoxical
286 results of significant interaction terms yet small increases in overall model R^2 , and comparably
287 much larger differences in R^2 in the stratified analyses.

288

289 Effects of machine learning approaches on predictive performance

290 Given evidence of PGS-covariate dependence, we aimed to assess increases in R^2 when using
291 machine learning models (neural networks), which can inherently model interactions and other
292 nonlinearities, over linear models even with interaction terms. We first included age and sex as
293 the only covariates (along with genotype PCs and PGS_{BMI}), as age and sex were present in all
294 datasets and had significant and replicable evidence for PGS-dependence across our analyses.
295 Three models were assessed – L1-regularized (i.e., LASSO) linear regression without any
296 interaction terms, LASSO including a PGS-age and PGS-sex interaction term, and neural
297 networks (without interaction terms). When comparing neural networks to LASSO with
298 interaction terms, the relative 10-fold cross-validated R^2 increased up to 67% (mean 23%) across
299 cohorts and ancestries (Figure 6, Supplemental Table 7). The inclusion of interaction terms
300 increased cross-validated R^2 up to 12% (mean 3.9%) when comparing LASSO including
301 interaction terms to LASSO with main effects only.

302 We then modeled all available covariates and their interactions with PGS for each cohort
303 and did similar comparisons. Cross-validated R^2 increased by up to 17.6% (mean 9.5%) when
304 using neural networks versus LASSO with interaction terms, and up to 7.0% (mean 2.0%) when
305 comparing LASSO with interaction terms to LASSO with main effects only. Increases in model
306 performance using neural networks were smaller in UKBB, perhaps due to the age range being
307 smaller than other cohorts (all participants aged 39-73). This result suggests that additional
308 variance explained through non-linear effects with age and sex are explained by other variables
309 present in the remainder of the datasets. Our findings show machine learning methods can
310 improve model R^2 that include PGS_{BMI} as variables beyond including interaction terms in linear
311 models, even when variable selection is performed using LASSO, demonstrating that model
312 performance can be increased beyond modeling nonlinearities through linear interaction terms
313 and a feature selection procedure.

314

315 Calculating PGS directly from GxAge GWAS effects

316 Previous studies (13) have created PGS using GWAS stratified by different personal-level
317 covariates, but for practical purposes this leads to a large loss of power as the full size of the
318 GWAS is not utilized for each strata and continuous variables are forced into bins. We developed
319 a novel strategy where PGS are instead created from a full-size GWAS that includes SNP-
320 covariate interaction terms (Methods). We focused on age interactions, given their large and
321 replicable effects based on our results – similar to a previous study (13), we conducted these
322 analyses in the European UKBB. We used a 60% random split of study individuals to conduct

323 three sets of PGS using GWAS of the following designs: main effects only, main effects also
324 with a SNP-age interaction term, and main effects but stratified into quartiles by age. 20% of the
325 remaining data were used for training and the final 20% were held-out as a test set. The best
326 performing PGS created from SNP-age interaction terms ($PGS_{G \times Age}$) increased test R^2 to 0.0771
327 (95% bootstrap CI: 0.0770-0.0772) from 0.0715 (95% bootstrap CI: 0.0714-0.0716), a 7.8%
328 relative increase compared to the best performing main effect PGS (Figure 7, Supplemental
329 Table 8 – age-stratified PGS had much lower performance than both other strategies
330 (unsurprising given reasons previously mentioned). Including a $PGS_{G \times Age}$ -age interaction term
331 only marginally increased R^2 (0.0001 increase), with similar increases for the other two sets of
332 PGS, further demonstrating that post-hoc modeling of interactions cannot reconcile performance
333 gained through directly incorporating interaction effects from the original GWAS. The strategy
334 of creating PGS directly from full-sized SNP-covariate interactions is potentially quite useful as
335 it increases PGS performance without the need for additional data – there are almost certainly a
336 variety of points of improvement (described more in Discussion), but we consider their
337 investigation outside the scope of this study.

338

339 Discussion

340 We uncovered replicable effects of covariates across four large-scale cohorts of diverse ancestry,
341 on both performance and effects of PGS_{BMI} . When stratifying by quintiles of different covariates,
342 certain covariates had significant and replicable evidence for differences in $PGS_{BMI} R^2$, with R^2
343 being nearly double between top and bottom performing quintiles for covariates with the largest
344 differences. When testing PGS-covariate interaction effects, we also found covariates with
345 significant interaction effects, where, for the largest effect covariates, each standard deviation
346 change affected PGS_{BMI} effect by nearly 20%. Across analyses, we found age and sex had the
347 most replicable interaction effects, with levels of serum cholesterol, physical activity, and
348 alcohol consumption having the largest effects across cohorts. Interaction effects and R^2
349 differences were strongly correlated, with main effects also being correlated with interaction
350 effects and R^2 differences, suggesting that covariates with the largest interaction effects also
351 contribute to the largest R^2 differences, with simple main effects also being predictive of
352 expected differences in R^2 and interaction effects. Relatedly, we observed the effect of PGS_{BMI}
353 increases as BMI itself increases, and reason that differences in R^2 when stratifying by covariates
354 are largely a consequence of difference in PGS_{BMI} effects. Next, we employed machine learning
355 methods for prediction of BMI with models that include PGS_{BMI} and demonstrate that these
356 methods outperform regularized linear regression models that include interaction effects. Finally,
357 we employed a novel strategy that directly incorporates SNP interaction effects into PGS
358 construction, and demonstrate that this strategy improves PGS performance when modeling
359 SNP-age interactions compared to PGS created only from main effects.

360 These observations are relevant to current research and clinical use of PGS, as individuals
361 above a percentile cutoff are designated high-risk (40), implying that individuals most at-risk for
362 obesity have both disproportionately higher predicted BMI and increased BMI prediction
363 performance compared to the general population. More broadly, these results may likely extend
364 to single variant effects instead of those aggregated into a PGS, which may inform the cause of
365 previous GxE discoveries – for instance, variants near *FTO* that interact with physical activity
366 discovered through GWAS of BMI are robust and well-documented. However, individuals
367 engaging in physical activity will generally have lower BMI than those that are sedentary, and
368 these results suggest it may not be the difference in physical activity that's driving the

369 interaction, rather the difference in BMI itself. This concept may also apply to other traits – for
370 instance, sex-specific analyses are commonly performed, and variants with differing effects
371 between males and females GWAS may largely be explained by phenotypic differences, rather
372 than any combination of biological or lifestyle differences.

373 Future work may include replicating these analyses across additional traits, and trying to
374 understand why these differences occur, as well as further exploring machine learning and deep
375 learning methods on other phenotypes to determine if this trend of inclusion of PGS along with
376 covariate interaction effects outperforms linear models for risk prediction. Additionally,
377 inclusion of a PGS for the covariate to better measure its environmental effect is potentially
378 worth exploring further, and should improve in the future as PGS performance continues to
379 increase. A slight limitation of this method in our study is that for the UKBB analyses the
380 GWAS used for PGS construction were also from UKBB thus not out-of-sample, although many
381 of the covariates only have GWAS available through UKBB individuals. Furthermore, a variety
382 of improvements are likely possible when creating PGS directly from SNP-covariate interaction
383 terms. First, we used the same SNPs that were selected by pruning and thresholding based on
384 their main effect p-values, but selection of SNPs based on their interaction p-values should also
385 be possible and would likely improve performance. Additionally, performance of pruning and
386 thresholding-based strategies have largely been overtaken by methods that first adjust all SNP
387 effects for LD and don't require exclusion of SNPs, and a method that could do a similar
388 adjustment for interaction effects would likely outperform most current methods for traits with
389 significant context-specific effects. Next, incorporating additional SNP-covariate interactions
390 (e.g., SNP-sex) would also likely further improve prediction performance, although any SNP
391 selection/adjustment procedures may be further complicated by additional interaction terms.
392 Finally, if SNP effects do truly differ according to differences in phenotype, then SNP effects
393 would differ depending on the alleles one has, implying epistatic interactions are occurring at
394 these SNPs.

395 While difference in phenotype itself may be able to explain difference in genetic effects,
396 it still may be that specific environmental or lifestyle characteristics are driving the differences.
397 We propose several ideas about why BMI-associated covariates have larger interaction effects
398 and impact on R^2 for PGS_{BMI} . First, age may be a proxy for accumulated gene-environment
399 interactions as younger individuals have less exposure to environmental influences on weight
400 compared to older individuals; therefore, one may expect that in younger individuals their
401 phenotype could be better explained by genetics compared to environment. Second, PGS may
402 more readily explain high phenotype values especially for positively skewed phenotypes, as
403 large effect variants (e.g., associated with very high weight or height (25)) may be more
404 responsible for extremely high phenotypic values. For example, the distribution of BMI is often
405 positively skewed, and effects in trait-increasing alleles may have a larger potential to explain
406 trait variation compared to trait-reducing variants. This explanation would likely be better suited
407 to positively skewed traits and is not fully satisfactory as first log-transforming or rank-normal
408 transforming the phenotype, as was done in this study, may invalidate this explanation.

409 PGS is a promising technique to stratify individuals for their risk of common, complex
410 disease. To achieve more accurate predictions as well as promote equity, further research is
411 required regarding PGS methods and assessments. This research provides firm evidence
412 supporting the context-specific nature of PGS and the impact of nonlinear covariate effects for
413 improving polygenic prediction of BMI, promoting equitable use of PGS across ancestries and
414 cohorts.

415

416 **Methods**

417 Study datasets

418 Individual inclusion criteria and sample sizes per cohort are described below – additional
419 information is available in Supplemental Table 1.

420

421 *UKBB*

422 Individual-level quality-control and filtering have been described elsewhere (26) for European
423 ancestry individuals. Briefly, individuals were split by ancestry according to both genetically
424 inferred ancestry and self-reported ethnicity (15). Individuals with low genotyping quality and
425 sex mismatch were removed, only unrelated individuals ($\pi\text{-hat} < 0.250$) were retained, and
426 variants were filtered at $\text{INFO} > 0.30$ and minor allele frequency (MAF) > 0.01 . For African
427 ancestry, individuals were first selected based on self-reported ethnicity “Black or Black
428 British”, “Caribbean”, “African”, or “Any other Black background”. Individuals that were low
429 quality i.e., “Outliers for heterozygosity or missing rate”, and that were Caucasian from “Genetic
430 ethnic grouping” were removed. Of these individuals, those that were ± 6 standard deviations
431 from the mean of the first 5 genetic principal components provided by UKBB were excluded.
432 Finally, only unrelated individuals were retained up to the second degree using plink2 (27) “-
433 king-cutoff 0.125”. After QC and consideration of phenotype, a total of 7,046 individuals in the
434 UKBB AFR data who also had BMI available were used for downstream analyses. In total,
435 383,775 individuals were used for analysis ($N_{\text{EUR}}=376,729$, $N_{\text{AFR}}=7,046$).

436

437 *eMERGE*

438 Ancestry and relatedness inference have been described elsewhere (15). Individuals were split
439 into European and African ancestry cohorts, and related individuals were removed ($\pi\text{-hat} >$
440 0.250) such that all were unrelated. 35,064 individuals ($N_{\text{EUR}}=31,961$, $N_{\text{AFR}}=3,103$) were used
441 for analysis.

442

443 *GERA*

444 Ancestry inference has been described elsewhere (28), and study individuals were divided into
445 European and African ancestry cohorts. Related individuals were removed using plink2 “-king-
446 cutoff 0.125”. 57,838 individuals ($N_{\text{EUR}}=56,049$, $N_{\text{AFR}}=1,789$) were used for analysis.

447

448 *PMBB*

449 Ancestry inference and relatedness inference have been described elsewhere (29). Individuals
450 were split into European and African ancestry cohorts, and related individuals were removed at
451 $\pi\text{-hat} > 0.250$. 36,046 individuals ($N_{\text{EUR}}=26,372$, $N_{\text{AFR}}=9,674$) were used for analysis.

452

453 Choice of covariates

454 A total of 62 covariates were included in the analyses, 25 of which were present (or similar
455 proxies) in multiple datasets. These covariates were selected based on relevance to
456 cardiometabolic health and obesity, and previous evidence of context-specific effects with BMI
457 (5,6,8,30–32). For UKBB, phenotype values were used from the collection that was closest to
458 recruitment, and for PMBB the median values were used – for GERA and eMERGE only one
459 value was available. Additional details on covariate constructions, transformations, filtering, and
460 cohort availability are in Supplemental Table 2.

461
462 PGS construction
463 PGS for BMI (PGS_{BMI}) were constructed using PRS-CSx (33), using GWAS summary statistics
464 for individuals of European (34), African (35), and East Asian (36) ancestry that were out-of-
465 sample of study participants. A set of 1.29 million HapMap3 SNPs provided by PRS-CSx was
466 used for PGS calculation, which are generally well-imputed and variable frequency across global
467 populations. Default settings for PRS-CSx (downloaded November 22, 2021) were used, which
468 have been demonstrated to perform well for highly polygenic traits such as BMI (list of
469 parameters in Supplemental Table 9). The final PGS_{BMI} per ancestry and cohort was calculated
470 by regressing $\log(BMI)$ on the PGS_{BMI} per ancestry without covariates – the combined, predicted
471 value was used as a single PGS_{BMI} in downstream analyses.

472
473 For GERA, BMI was not transformed, as it was already binned into a categorical variable with 5
474 levels ($18 \leq$, 19-25, 26-29, 30-39, >40). Additionally, for GERA the uncombined ancestry-
475 specific PGS_{BMI} were used in the final models, as it had higher R^2 than using the combined
476 PGS_{BMI} (data not shown).

477 PGS_{BMI} performance after covariate stratification

478 Analyses were performed separately for each cohort and ancestry. For each covariate, individuals
479 were binned by binary covariates or quintiles for continuous covariates. Incremental PGS_{BMI} R^2
480 was calculated by taking the difference in R^2 between:
481

$$482 \log(BMI) \sim PGS_{BMI} + Age + Sex + PCs_{1-5}$$

$$483 \log(BMI) \sim Age + Sex + PCs_{1-5}$$

484
485
486 We performed 5,000 bootstrap replications to obtain a bootstrapped distribution of R^2 . P-values
487 for differences in R^2 were calculated between groups by calculating the proportion of overlap
488 between two normal distributions of the R^2 value using the standard deviations of the bootstrap
489 distributions. Again for GERA, BMI was not transformed.

490 PGS_{BMI} interaction modelling

491 Evidence for interaction with each covariate with the PGS_{BMI} was evaluated using linear
492 regression. It has been reported that the inclusion of covariates that are genetically correlated
493 with the outcome can inflate test statistic estimates (24,37,38). To assuage these concerns, we
494 introduced a novel correction, where we first calculated a PGS for the covariate ($PGS_{Covariate}$) and
495 included it in the model, as well as an interaction term between PGS_{BMI} and $PGS_{Covariate}$. The
496 $PGS_{Covariate}$ terms were calculated using the European ancestry Neale Lab summary statistics
497 (URLs) and PRS-CS (39). To standardize effect sizes across analyses, PGS_{BMI} and Covariate
498 were first converted to mean zero and standard deviation of 1 (binary covariates were not
499 standardized). We demonstrate inclusion of $PGS_{Covariate}$ terms successfully reduced significance
500 of the $PGS_{BMI} * Covariate$ term (Supplemental Figure 1). The final model used to evaluate
501 PGS_{BMI} and Covariate interactions was:
502

$$503 \log(BMI) \sim PGS_{BMI} * Covariate + PGS_{BMI} + Covariate + PGS_{Covariate} + PGS_{BMI} * PGS_{Covariate} + Age + Sex + PCs_{1-5}$$

504
505
506 We report the effect estimates of the $PGS_{BMI} * Covariate$ term, and differences in model R^2 with
507 and without the $PGS_{BMI} * Covariate$ term. Again for GERA, BMI was not transformed.

508

509 Correlation between R^2 differences, interaction effects, and main effects

510 We estimated main effects of each covariate on BMI with the following model:

511

$$512 \log(\text{BMI}) \sim \text{Covariate} + \text{Age} + \text{Sex} + \text{PC}_{\text{S}_{1-5}}$$

513

514 Note that we ran new models with main effects only, instead of using the main effect from the
515 interaction models (as the main effects in the interaction models depend on the interaction terms,
516 and main effects used to create interaction terms are sensitive to centering of variables despite
517 the scale invariance of linear regression itself (40)). We then estimated the correlation between
518 main effects, interaction effects, and maximum R^2 differences across all cohorts and ancestries
519 weighting by sample size, analyzing quantitative and binary variables separately.

520

521 Quantile regression to measure PGS effect across percentiles of BMI

522 The effect of PGS_{BMI} on BMI at different deciles of BMI was assessed using quantile regression.

523 Tau – the parameter that sets which percentile to be predicted – was set to .10, .20, ..., .90.

524 Models included age, sex, and the top 5 genetic PCs as covariates. Analyses were stratified by
525 ancestry and cohort, and BMI was first log transformed. GERA was excluded from these
526 analyses, as a portion of the models failed to run (as BMI values from GERA were already
527 binned, some deciles all had the same BMI value – additionally, difference in effects between
528 bins would be harder to evaluate as BMI within each decile would be more homogeneous).

529

530 Machine learning models

531 UKBB EUR and GERA EUR models were restricted to 30,000 random individuals, for
532 computational reasons – BMI distributions did not differ from the full-sized datasets
533 (Kolmogorov-Smirnov p-value of 0.29 and 0.57, respectively). PGS_{BMI} and top five genetic
534 principal components were included as features in all models. Two sets of models were
535 evaluated for each cohort and ancestry: including age and sex as features, and including all
536 available covariates in each cohort as features. Interactions terms between PGS and each
537 covariate were included for models using interaction terms. ‘Ever Smoker’ status was used in
538 favor of ‘Never’ vs ‘Current smoking’ status (if present), as individuals with ‘Never’ vs
539 ‘Current’ status are a subset of those with ‘Ever Smoker’ status. UKBB AFR with all covariates
540 was excluded due to small sample size (N=53).

541 Neural networks were used as the model of choice, given their inherent ability model
542 interactions and other nonlinear dependencies. Prior to modeling, all features were scaled to be
543 between 0 and 1. We used average 10-fold cross validation R^2 to evaluate model performance.
544 Separate models were trained using untransformed and $\log(\text{BMI})$. L1-regularized linear
545 regression was used with 18 values of lambda (1.0 , 5.0×10^{-1} , 2.0×10^{-1} , 1.0×10^{-1} , 5.0×10^{-2} , 2.0×10^{-2} ,
546 1.0×10^{-5} , 5.0×10^{-6} , 2.0×10^{-6}). Models were trained without inclusion of interaction terms
547 (which neural networks can implicitly model), using 1,000 iterations of random search with the
548 following hyperparameter ranges: size of hidden layers [10, 200], learning rate [0.01, 0.0001],
549 type of learning rate [constant, inverse scaling], power t [0.4, 0.6], momentum [0.80, 1.0], batch
550 size [32, 256], and number of hidden layers [1, 2].

551

552 GxAge PGS_{BMI} creation and assessment

553 Analyses were conducted in the European UKBB (N=376,629), as was done in a study on a
554 similar topic (13). Three sets of analyses were performed, using GWAS conducted in a 60%

555 random split of individuals using the following models (BMI was rank-normal transformed
556 before GWAS):

- 557
- 558 1) $BMI \sim SNP + Age + Sex + PC_{S1-5}$
 - 559
 - 560 2) $BMI \sim SNP + Age * SNP + Age + Sex + PC_{S1-5}$
 - 561
 - 562 3) Using the model in 1) but stratified into quartiles by age. BMI was rank-normal transformed
563 within each quartile.

564

565 Using each set of GWAS, PGS was first calculated in a 20% randomly selected training set of
566 the dataset using pruning and thresholding using 10 p-value thresholds ($0.50, 0.10, \dots, 5.0 \times 10^{-5},$
567 1.0×10^{-5}) and remaining settings as default in Plink 1.9. For 2), GxAge PGS_{BMI} were calculated
568 using SNPs clumped by their main effect p-values from 1), and additionally incorporating the
569 GxAge interaction effects per SNP. In other words, instead of typical PGS construction as:

570

$$571 PGS_i = \beta_1 k_1 + \beta_2 k_2 + \dots + \beta_n k_n$$

572

573 For an individual i 's PGS calculation, with main SNP effect β , and n SNPs, PGS incorporating
574 GxAge effects (PGS_{GxAge}) was calculated as:

575

$$576 PGS_{GxAge,i} = \beta_1 k_1 + \beta_{GxAge,1} k_1 Age_i + \beta_2 k_2 + \beta_{GxAge,2} k_2 Age_i \dots + \beta_n k_n + \beta_{GxAge,n} k_n Age_i$$

577

578 Where β_{GxAge} is the GxAge effect for each SNP n and Age_i is the age for individual i .

579

580 For each of the three analyses, the parameters and models resulting in the best performing PGS
581 (highest incremental R^2 , using same main effect covariates as in the three GWAS) from the
582 training set were evaluated in the remaining 20% of the study individuals. For 3), models were
583 first trained within each quartile separately. To maintain sense of scale across quartiles (after
584 rank-normal transformation), R^2 between all predicted values and true values was calculated
585 together. For R^2 confidence intervals, the training set was bootstrapped and evaluated on the test
586 set 5,000 times.

587

588 **URLs**

589 Neale Lab UKBB summary statistics: <http://www.nealelab.is/uk-biobank>

590

591 **Data Availability statement**

592 UK Biobank data was accessed under project #32133. eMERGE data is available at dbGaP in
593 phs001584.v2.p2. GERA data is available at dbGaP in phs000674.v3.p3. Summary statistics for
594 PMBB are available from authors upon request.

595

596 **Regeneron Genetics Center Banner Author List and Contribution Statements**

597 RGCC Management and Leadership Team

598 Goncalo Abecasis, PhD, Aris Baras, M.D., Michael Cantor, M.D., Giovanni Coppola, M.D.,
599 Andrew Deubler, Aris Economides, Ph.D., Luca A. Lotta, M.D., Ph.D., John D. Overton, Ph.D.,
600 , Jeffrey G. Reid, Ph.D., Katherine Siminovitch, M.D., Alan Shuldiner, M.D.

601
602
603
604
605
606
607
608
609
610
611
612
613
614
615
616
617
618
619
620
621
622
623
624
625
626
627
628
629
630
631
632
633
634
635
636
637
638
639
640
641
642
643
644
645

Sequencing and Lab Operations

Christina Beechert, Caitlin Forsythe, M.S., Erin D. Fuller, Zhenhua Gu, M.S., Michael Lattari, Alexander Lopez, M.S., John D. Overton, Ph.D., Maria Sotiropoulos Padilla, M.S., Manasi Pradhan, M.S., Kia Manoochehri, B.S., Thomas D. Schleicher, M.S., Louis Widom, Sarah E. Wolf, M.S., Ricardo H. Ulloa, B.S.

Clinical Informatics

Amelia Averitt, Ph.D., Nilanjana Banerjee, Ph.D., Michael Cantor, M.D., Dadong Li, Ph.D., Sameer Malhotra, M.D., Deepika Sharma, MHI, Jeffrey Staples, Ph.D.

Genome Informatics

Xiaodong Bai, Ph.D., Suganthi Balasubramanian, Ph.D., Suying Bao, Ph.D., Boris Boutkov, Ph.D., Siying Chen, Ph.D., Gisu Eom, B.S., Lukas Habegger, Ph.D., Alicia Hawes, B.S., Shareef Khalid, Olga Krasheninina, M.S., Rouel Lanche, B.S., Adam J. Mansfield, B.A., Evan K. Maxwell, Ph.D., George Mitra, B.A., Mona Nafde, M.S., Sean O’Keeffe, Ph.D., Max Orelus, B.B.A., Razvan Panea, Ph.D., Tommy Polanco, B.A., Ayesha Rasool, M.S., Jeffrey G. Reid, Ph.D., William Salerno, Ph.D., Jeffrey C. Staples, Ph.D., Kathie Sun, Ph.D.

Analytical Genomics and Data Science

Goncalo Abecasis, D.Phil., Joshua Backman, Ph.D., Amy Damask, Ph.D., Lee Dobbyn, Ph.D., Manuel Allen Revez Ferreira, Ph.D., Arkopravo Ghosh, M.S., Christopher Gillies, Ph.D., Lauren Gurski, B.S., Eric Jorgenson, Ph.D., Hyun Min Kang, Ph.D., Michael Kessler, Ph.D., Jack Kosmicki, Ph.D., Alexander Li, Ph.D., Nan Lin, Ph.D., Daren Liu, M.S., Adam Locke, Ph.D., Jonathan Marchini, Ph.D., Anthony Marcketta, M.S., Joelle Mbatchou, Ph.D., Arden Moscati, Ph.D., Charles Paulding, Ph.D., Carlo Sidore, Ph.D., Eli Stahl, Ph.D., Kyoko Watanabe, Ph.D., Bin Ye, Ph.D., Blair Zhang, Ph.D., Andrey Ziyatdinov, Ph.D.

Therapeutic Area Genetics

Ariane Ayer, B.S., Aysegul Guvenek, Ph.D., George Hindy, Ph.D., Giovanni Coppola, M.D., Jan Freudenberg, M.D., Jonas Bovijn M.D., Katherine Siminovitch, M.D., Kavita Praveen, Ph.D., Luca A. Lotta, M.D., Manav Kapoor, Ph.D., Mary Haas, Ph.D., Moeen Riaz, Ph.D., Niek Verweij, Ph.D., Olukayode Sosina, Ph.D., Parsa Akbari, Ph.D., Priyanka Nakka, Ph.D., Sahar Gelfman, Ph.D., Sujit Gokhale, B.E., Tanima De, Ph.D., Veera Rajagopal, Ph.D., Alan Shuldiner, M.D., Bin Ye, Ph.D., Gannie Tzoneva, Ph.D., Juan Rodriguez-Flores, Ph.D.

Research Program Management & Strategic Initiatives

Esteban Chen, M.S., Marcus B. Jones, Ph.D., Michelle G. LeBlanc, Ph.D., Jason Mighty, Ph.D., Lyndon J. Mitnaul, Ph.D., Nirupama Nishtala, Ph.D., Nadia Rana, Ph.D., Jaimee Hernandez

Acknowledgements

We acknowledge David Crosslin for helping clean the eMERGE data.

Funding

646 M.D.R., S.D., and D.H. are funded by AI077505 and HL169458. W.K.C is funded by grant
647 NIDDK DK52431. J.F.P. is funded by grant U01 HG011166. C.W. is funded by U01
648 HG008680. This phase of the eMERGE Network was initiated and funded by the NHGRI
649 through the following grants: U01HG008657 (Group Health Cooperative/University of
650 Washington); U01HG008685 (Brigham and Women's Hospital); U01HG008672 (Vanderbilt
651 University Medical Center); U01HG008666 (Cincinnati Children's Hospital Medical Center);
652 U01HG006379 (Mayo Clinic); U01HG008679 (Geisinger Clinic); U01HG008680 (Columbia
653 University Health Sciences); U01HG008684 (Children's Hospital of Philadelphia);
654 U01HG008673 (Northwestern University); U01HG008701 (Vanderbilt University Medical
655 Center serving as the Coordinating Center); U01HG008676 (Partners Healthcare/Broad
656 Institute); U01HG008664 (Baylor College of Medicine); and U54MD007593 (Meharry Medical
657 College).

658 **References**

- 660 1. Martin AR, Kanai M, Kamatani Y, Okada Y, Neale BM, Daly MJ. Clinical use of current
661 polygenic risk scores may exacerbate health disparities. *Nat Genet.* 2019 Apr;51(4):584–91.
- 662 2. Wang Y, Guo J, Ni G, Yang J, Visscher PM, Yengo L. Theoretical and empirical
663 quantification of the accuracy of polygenic scores in ancestry divergent populations. *Nat*
664 *Commun.* 2020 Jul 31;11(1):3865.
- 665 3. Galinsky KJ, Reshef YA, Finucane HK, Loh PR, Zaitlen N, Patterson NJ, et al. Estimating
666 cross-population genetic correlations of causal effect sizes. *Genet Epidemiol.* 2019
667 Mar;43(2):180–8.
- 668 4. Shi H, Gazal S, Kanai M, Koch EM, Schoech AP, Siewert KM, et al. Population-specific
669 causal disease effect sizes in functionally important regions impacted by selection. *Nat*
670 *Commun.* 2021 Feb 17;12(1):1098.
- 671 5. Rask-Andersen M, Karlsson T, Ek WE, Johansson Å. Gene-environment interaction study
672 for BMI reveals interactions between genetic factors and physical activity, alcohol
673 consumption and socioeconomic status. *PLoS Genet.* 2017 Sep;13(9):e1006977.
- 674 6. Robinson MR, English G, Moser G, Lloyd-Jones LR, Triplett MA, Zhu Z, et al. Genotype-
675 covariate interaction effects and the heritability of adult body mass index. *Nat Genet.* 2017
676 Aug;49(8):1174–81.
- 677 7. Sulc J, Mounier N, Günther F, Winkler T, Wood AR, Frayling TM, et al. Quantification of
678 the overall contribution of gene-environment interaction for obesity-related traits. *Nat*
679 *Commun.* 2020 Mar 13;11(1):1385.
- 680 8. Justice AE, Winkler TW, Feitosa MF, Graff M, Fisher VA, Young K, et al. Genome-wide
681 meta-analysis of 241,258 adults accounting for smoking behaviour identifies novel loci for
682 obesity traits. *Nat Commun.* 2017 Apr 26;8:14977.
- 683 9. Helgeland Ø, Vaudel M, Juliusson PB, Lingaas Holmen O, Juodakis J, Bacelis J, et al.
684 Genome-wide association study reveals dynamic role of genetic variation in infant and early
685 childhood growth. *Nat Commun.* 2019 Oct 1;10(1):4448.

- 686 10. Vogelezang S, Bradfield JP, Ahluwalia TS, Curtin JA, Lakka TA, Grarup N, et al. Novel loci
687 for childhood body mass index and shared heritability with adult cardiometabolic traits.
688 PLoS Genet. 2020 Oct;16(10):e1008718.
- 689 11. Couto Alves A, De Silva NMG, Karhunen V, Sovio U, Das S, Taal HR, et al. GWAS on
690 longitudinal growth traits reveals different genetic factors influencing infant, child, and adult
691 BMI. Sci Adv. 2019 Sep;5(9):eaaw3095.
- 692 12. Choh AC, Lee M, Kent JW, Diego VP, Johnson W, Curran JE, et al. Gene-by-age effects on
693 BMI from birth to adulthood: the Fels Longitudinal Study. Obes Silver Spring Md. 2014
694 Mar;22(3):875–81.
- 695 13. Mostafavi H, Harpak A, Agarwal I, Conley D, Pritchard JK, Przeworski M. Variable
696 prediction accuracy of polygenic scores within an ancestry group. eLife. 2020 Jan
697 30;9:e48376.
- 698 14. Elks CE, den Hoed M, Zhao JH, Sharp SJ, Wareham NJ, Loos RJF, et al. Variability in the
699 heritability of body mass index: a systematic review and meta-regression. Front Endocrinol.
700 2012;3:29.
- 701 15. Bycroft C, Freeman C, Petkova D, Band G, Elliott LT, Sharp K, et al. The UK Biobank
702 resource with deep phenotyping and genomic data. Nature. 2018 Oct;562(7726):203–9.
- 703 16. Stanaway IB, Hall TO, Rosenthal EA, Palmer M, Naranbhai V, Knevel R, et al. The
704 eMERGE genotype set of 83,717 subjects imputed to ~40 million variants genome wide
705 and association with the herpes zoster medical record phenotype. Genet Epidemiol. 2019
706 Feb;43(1):63–81.
- 707 17. Kilpeläinen TO, Qi L, Brage S, Sharp SJ, Sonestedt E, Demerath E, et al. Physical activity
708 attenuates the influence of FTO variants on obesity risk: a meta-analysis of 218,166 adults
709 and 19,268 children. PLoS Med. 2011 Nov;8(11):e1001116.
- 710 18. Rampersaud E, Mitchell BD, Pollin TI, Fu M, Shen H, O’Connell JR, et al. Physical activity
711 and the association of common FTO gene variants with body mass index and obesity. Arch
712 Intern Med. 2008 Sep 8;168(16):1791–7.
- 713 19. Amin V, Dunn P, Spector T. Does education attenuate the genetic risk of obesity? Evidence
714 from U.K. Twins. Econ Hum Biol. 2018 Sep;31:200–8.
- 715 20. Li Y, Cai T, Wang H, Guo G. Achieved educational attainment, inherited genetic
716 endowment for education, and obesity. Biodemography Soc Biol. 2021 Jun;66(2):132–44.
- 717 21. Frank M, Dragano N, Arendt M, Forstner AJ, Nöthen MM, Moebus S, et al. A genetic sum
718 score of risk alleles associated with body mass index interacts with socioeconomic position
719 in the Heinz Nixdorf Recall Study. PloS One. 2019;14(8):e0221252.
- 720 22. Ge T, Chen CY, Neale BM, Sabuncu MR, Smoller JW. Phenome-wide heritability analysis
721 of the UK Biobank. PLoS Genet. 2017 Apr;13(4):e1006711.

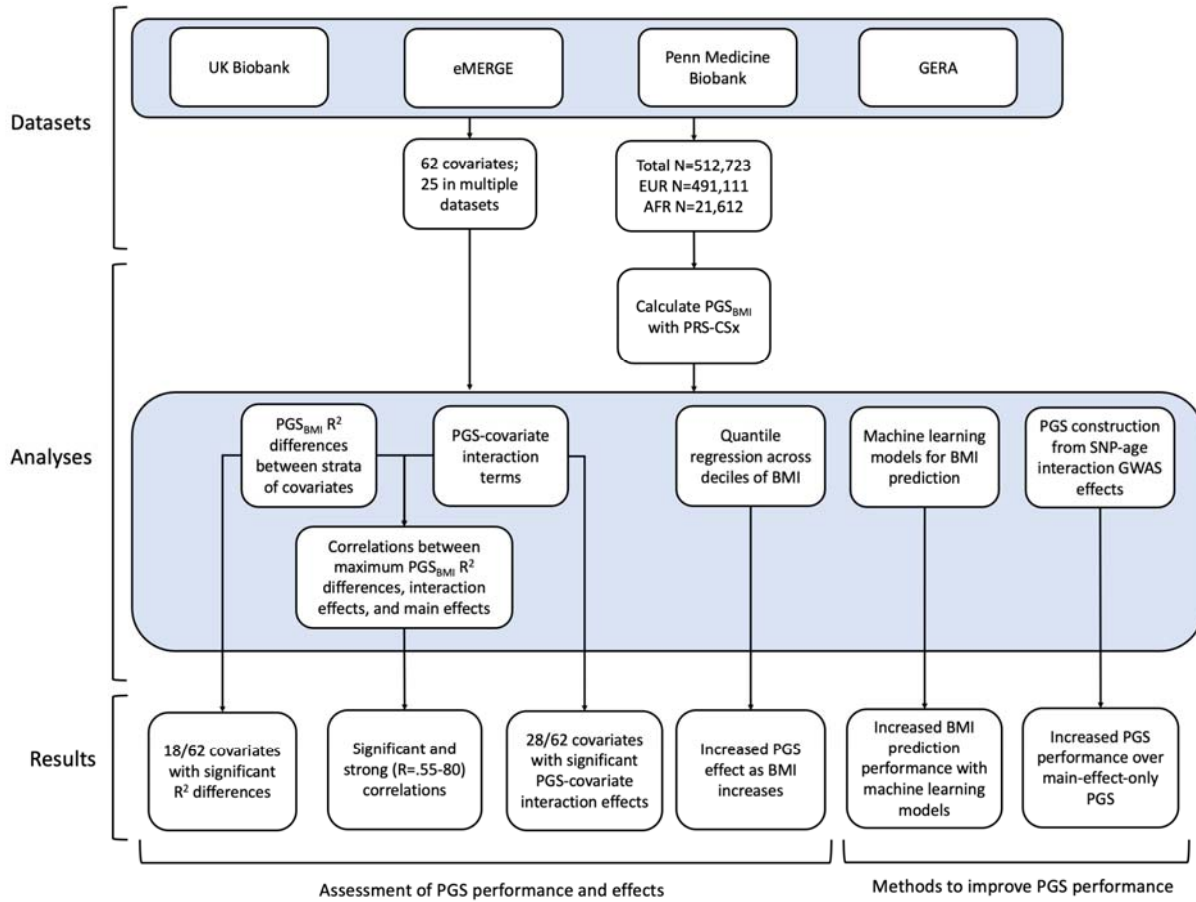
- 722 23. Min J, Chiu DT, Wang Y. Variation in the heritability of body mass index based on diverse
723 twin studies: a systematic review. *Obes Rev Off J Int Assoc Study Obes*. 2013
724 Nov;14(11):871–82.
- 725 24. Aschard H, Vilhjálmsson BJ, Joshi AD, Price AL, Kraft P. Adjusting for heritable covariates
726 can bias effect estimates in genome-wide association studies. *Am J Hum Genet*. 2015 Feb
727 5;96(2):329–39.
- 728 25. Robinson PN, Arteaga-Solis E, Baldock C, Collod-Bérout G, Booms P, De Paepe A, et al.
729 The molecular genetics of Marfan syndrome and related disorders. *J Med Genet*. 2006
730 Oct;43(10):769–87.
- 731 26. Zhang X, Lucas AM, Veturi Y, Drivas TG, Bone WP, Verma A, et al. Large-scale genomic
732 analyses reveal insights into pleiotropy across circulatory system diseases and nervous
733 system disorders. *Nat Commun*. 2022 Jun 14;13(1):3428.
- 734 27. Chang CC, Chow CC, Tellier LC, Vattikuti S, Purcell SM, Lee JJ. Second-generation
735 PLINK: rising to the challenge of larger and richer datasets. *GigaScience*. 2015;4:7.
- 736 28. Banda Y, Kvale MN, Hoffmann TJ, Hesselson SE, Ranatunga D, Tang H, et al.
737 Characterizing Race/Ethnicity and Genetic Ancestry for 100,000 Subjects in the Genetic
738 Epidemiology Research on Adult Health and Aging (GERA) Cohort. *Genetics*. 2015
739 Aug;200(4):1285–95.
- 740 29. Penn Medicine BioBank [Internet]. Available from: <https://pmbb.med.upenn.edu/>
- 741 30. Tyrrell J, Wood AR, Ames RM, Yaghootkar H, Beaumont RN, Jones SE, et al. Gene-
742 obesogenic environment interactions in the UK Biobank study. *Int J Epidemiol*. 2017 Apr
743 1;46(2):559–75.
- 744 31. Young AI, Wauthier F, Donnelly P. Multiple novel gene-by-environment interactions modify
745 the effect of FTO variants on body mass index. *Nat Commun*. 2016 Sep 6;7:12724.
- 746 32. Winkler TW, Justice AE, Graff M, Barata L, Feitosa MF, Chu S, et al. The Influence of Age
747 and Sex on Genetic Associations with Adult Body Size and Shape: A Large-Scale Genome-
748 Wide Interaction Study. *PLoS Genet*. 2015 Oct;11(10):e1005378.
- 749 33. Ruan Y, Lin YF, Feng YCA, Chen CY, Lam M, Guo Z, et al. Improving polygenic
750 prediction in ancestrally diverse populations. *Nat Genet*. 2022 May;54(5):573–80.
- 751 34. Locke AE, Kahali B, Berndt SI, Justice AE, Pers TH, Day FR, et al. Genetic studies of body
752 mass index yield new insights for obesity biology. *Nature*. 2015 Feb 12;518(7538):197–206.
- 753 35. Ng MCY, Graff M, Lu Y, Justice AE, Mudgal P, Liu CT, et al. Discovery and fine-mapping
754 of adiposity loci using high density imputation of genome-wide association studies in
755 individuals of African ancestry: African Ancestry Anthropometry Genetics Consortium.
756 *PLoS Genet*. 2017 Apr;13(4):e1006719.

- 757 36. Sakaue S, Kanai M, Tanigawa Y, Karjalainen J, Kurki M, Koshihara S, et al. A cross-
758 population atlas of genetic associations for 220 human phenotypes. *Nat Genet.* 2021
759 Oct;53(10):1415–24.
- 760 37. Kerin M, Marchini J. Inferring Gene-by-Environment Interactions with a Bayesian Whole-
761 Genome Regression Model. *Am J Hum Genet.* 2020 Oct 1;107(4):698–713.
- 762 38. Vanderweele TJ, Ko YA, Mukherjee B. Environmental confounding in gene-environment
763 interaction studies. *Am J Epidemiol.* 2013 Jul 1;178(1):144–52.
- 764 39. Ge T, Chen CY, Ni Y, Feng YCA, Smoller JW. Polygenic prediction via Bayesian regression
765 and continuous shrinkage priors. *Nat Commun.* 2019 Apr 16;10(1):1776.
- 766 40. Afshartous D, Preston RA. Key Results of Interaction Models with Centering. *J Stat Educ.*
767 2011 Nov;19(3):1.

768
769
770
771
772
773
774
775
776
777
778
779
780
781
782
783
784
785
786
787
788
789
790
791

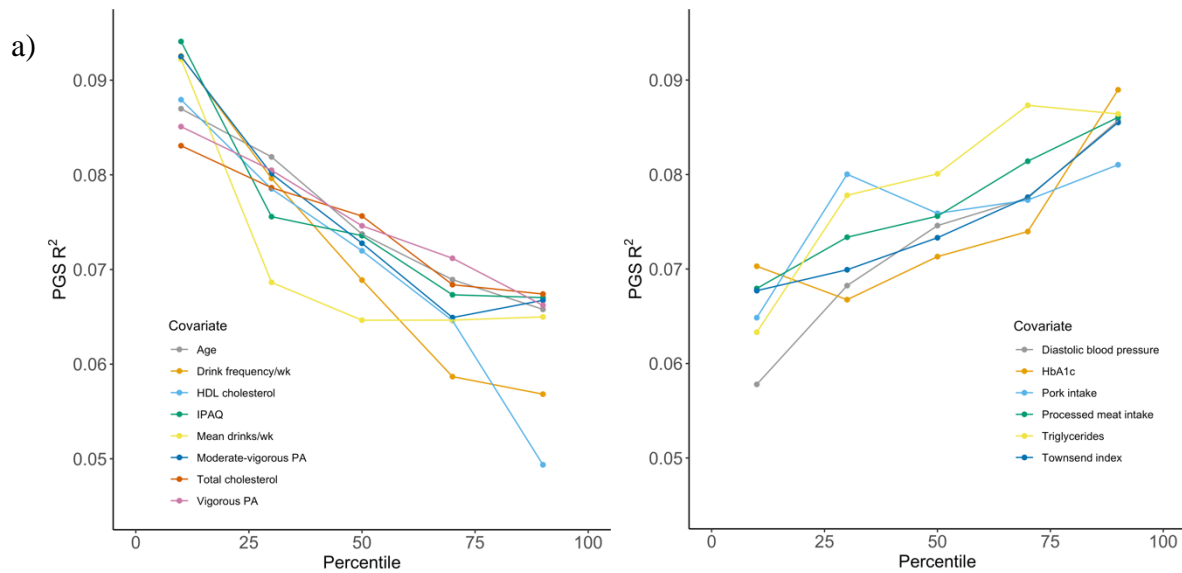
Figures

792

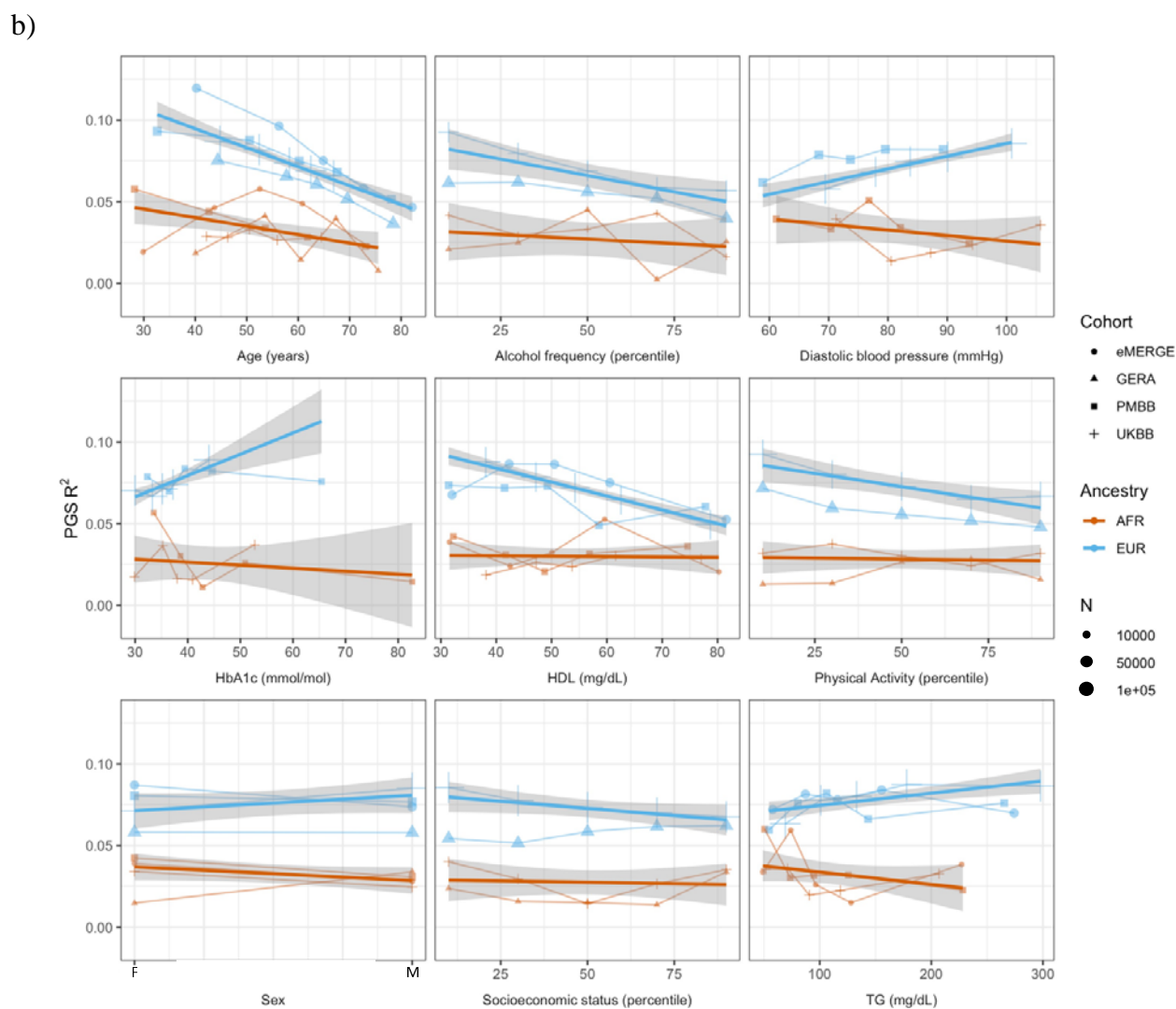


793
794
795
796
797
798
799
800
801
802
803
804
805

Figure 1. A flowchart of the project.

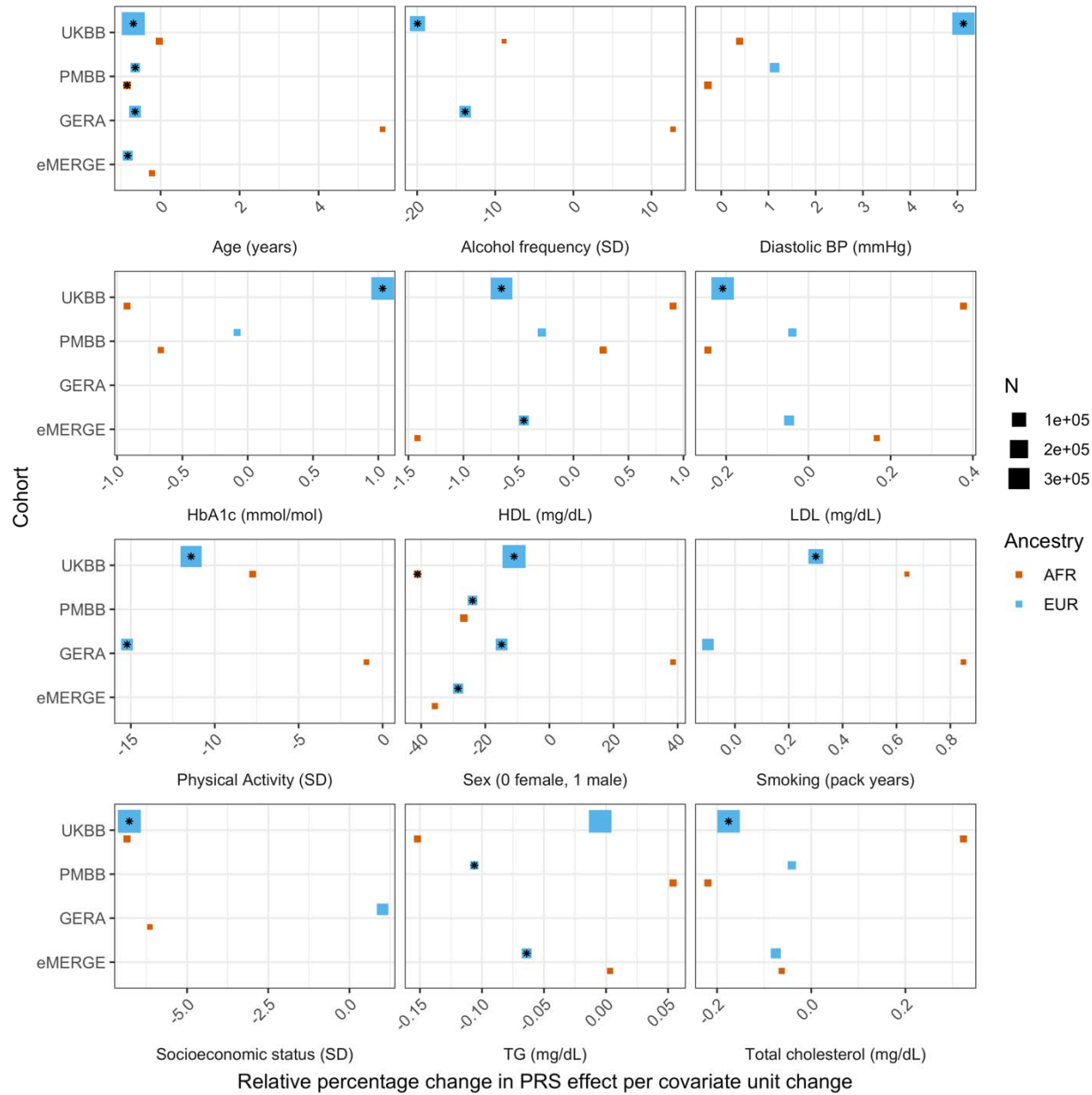


806
807
808



809
810

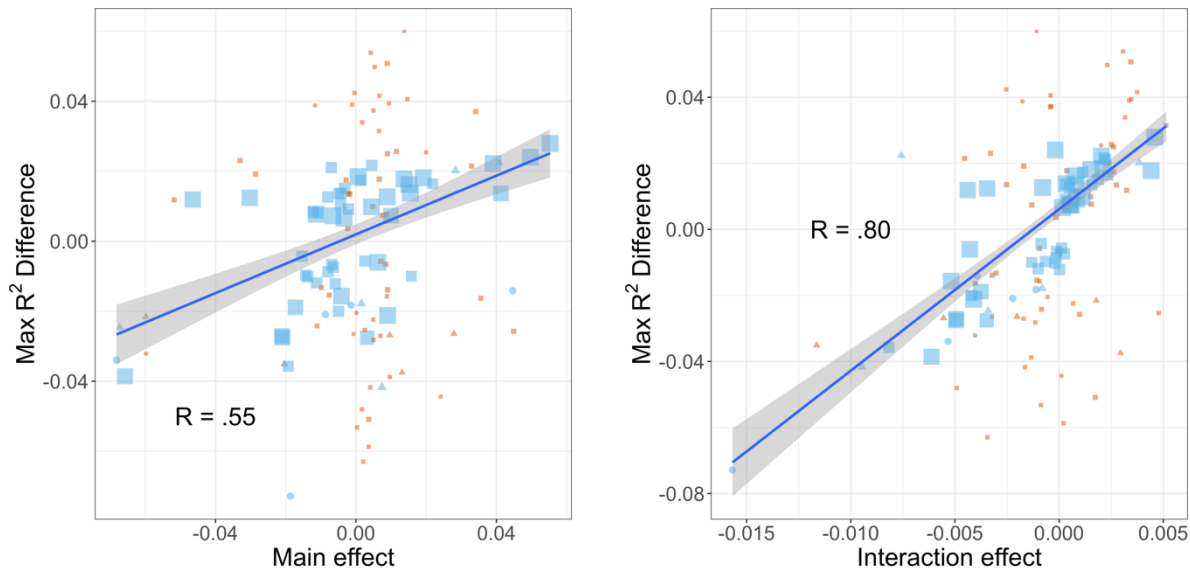
811 Figure 2. PGS R^2 stratified by quintiles for quantitative variables and by binary variables. a)
812 Continuous covariates with significant ($p < 8.1 \times 10^{-4}$) R^2 differences across quintiles in UKBB
813 EUR. Pork and processed meat consumption per week were excluded from this plot in favor of
814 pork and processed meat intake. b) Covariates with significant differences that were available in
815 multiple cohorts. When traits had the same or directly comparable units between cohorts we
816 show the actual trait values (and show percentiles for physical activity, alcohol intake frequency,
817 and socioeconomic status, which had slightly differing phenotype definitions across cohorts)
818 plotted on x-axis. Townsend index and income were used as variables for socioeconomic status
819 UKBB and GERA, respectively. Note that the sign for Townsend index was reversed, since
820 increasing Townsend index is lower socioeconomic status, while increasing income is higher
821 socioeconomic status. Abbreviations: physical activity (PA), International Physical Activity
822 Questionnaire (IPAQ).
823
824
825
826
827
828
829
830



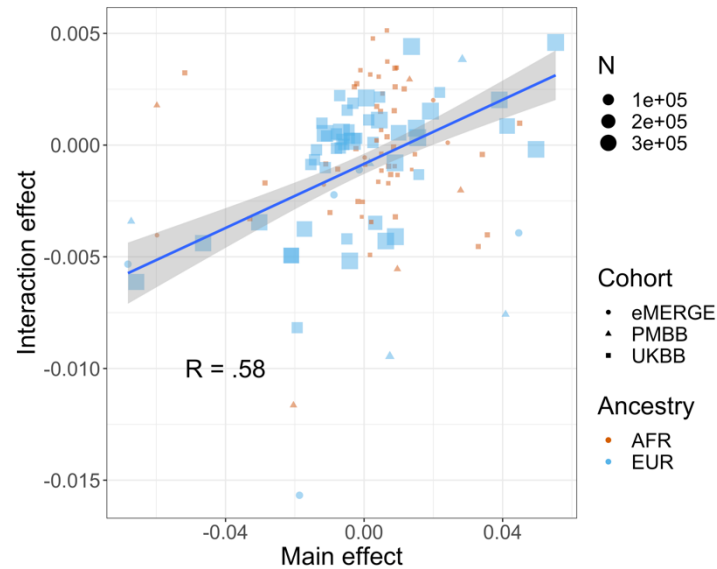
831
832
833
834
835
836
837
838
839
840
841
842
843
844

Figure 3. Relative percentage changes in PGS effect per unit change in covariate, for covariates that significantly changed PGS effect (i.e., significant interaction beta at Bonferroni $p < 8.1 \times 10^{-4}$ – denoted by asterisks) and were present in multiple cohorts and ancestries. Same covariate groupings and transformations were performed as in Figure 1. Similarly, actual values were used when variables had comparable units across cohorts, and standard deviations (SD) used otherwise.

845



846



847

848

849 Figure 4. Relationships (Pearson correlations weighted by sample size) between maximum R²
850 differences across strata, main effects of covariate on log(BMI), and PGS-covariate interaction
851 effects on log(BMI). Main effect units are in standard deviations, interaction effect units are in
852 PGS standard deviations multiplied by covariate standard deviations. Only continuous variables
853 are plotted and modeled. GERA was excluded due to slightly different phenotype definitions.

854

855

856

857

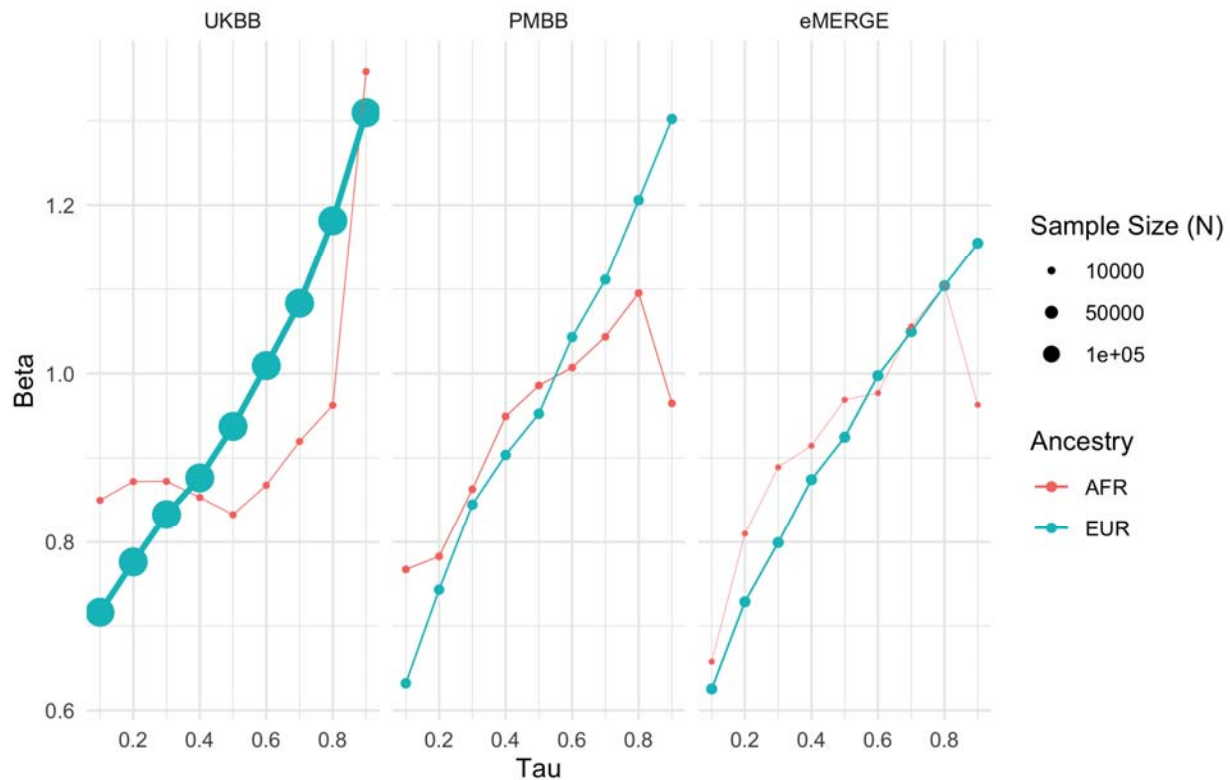
858

859

860

861

862



863

864

865

866

867

868

869

870

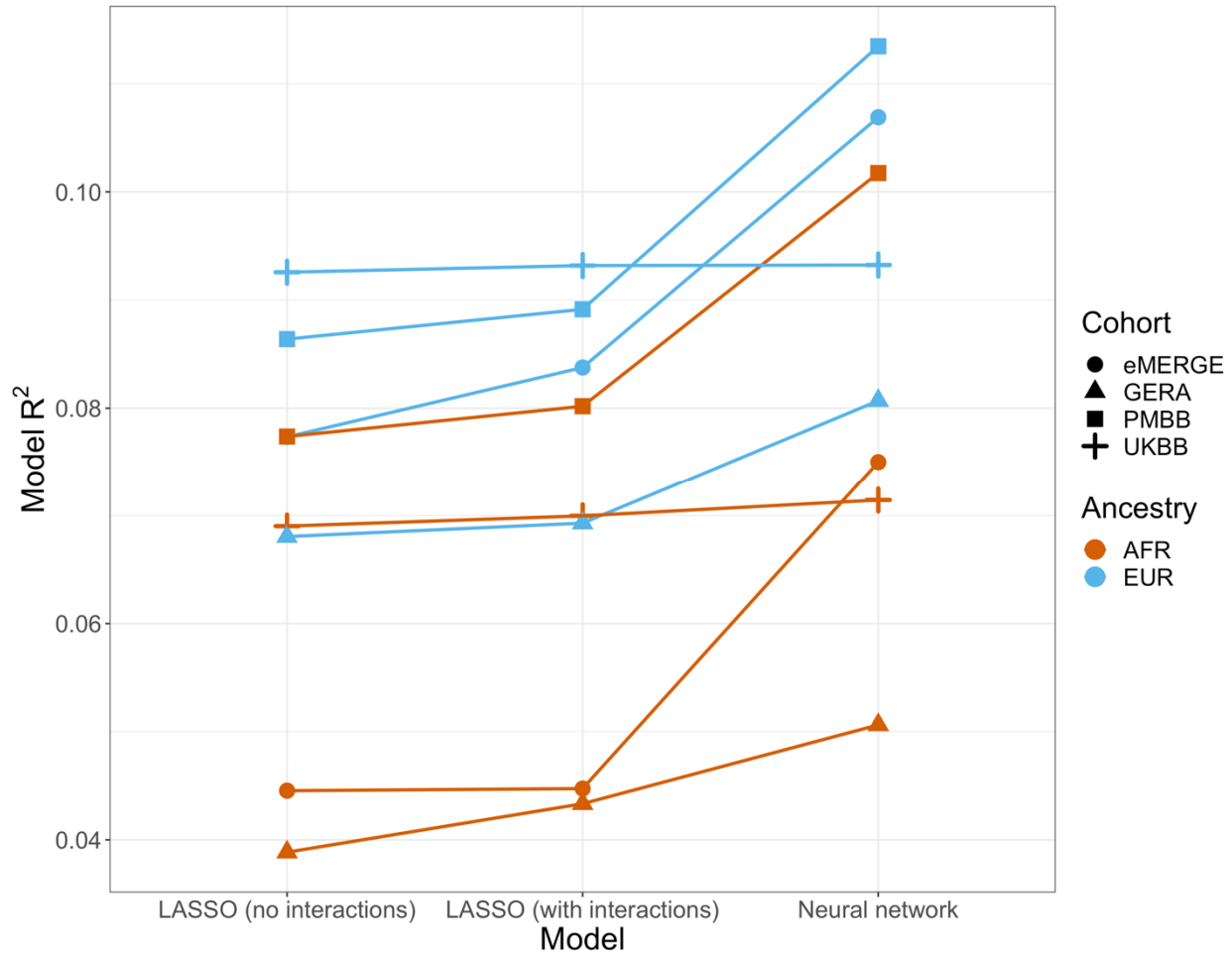
871

872

873

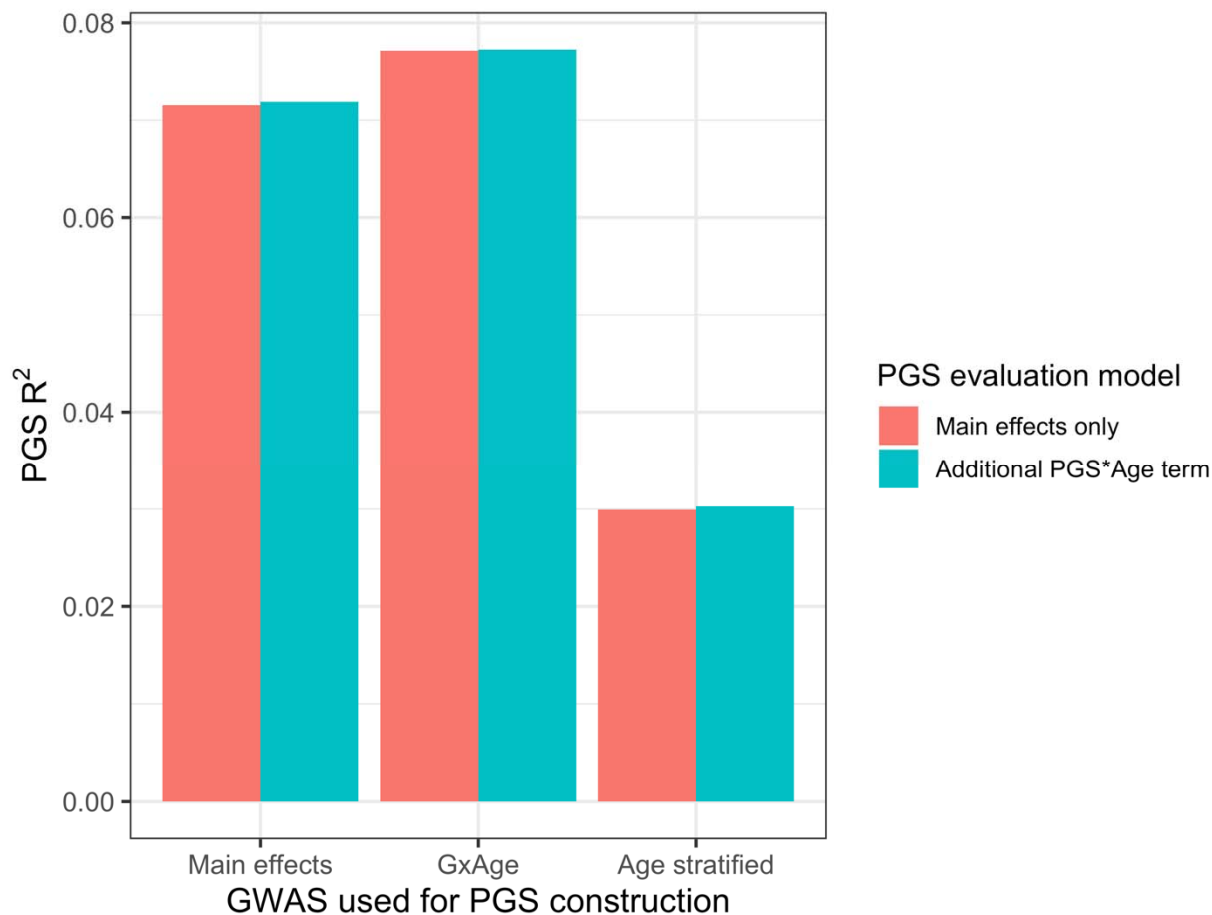
874

Figure 5. Quantile regression effects of PGS_{BMI} (in units of $\log(BMI)$) on $\log(BMI)$ at each decile of BMI in each cohort and ancestry. The effect of PGS_{BMI} increases as BMI itself increases, suggesting that no individual covariate-PGS interaction is responsible for the nonlinear effect of PGS_{BMI} .



875
876
877
878
879
880
881
882
883
884
885
886
887
888
889
890
891
892
893
894
895

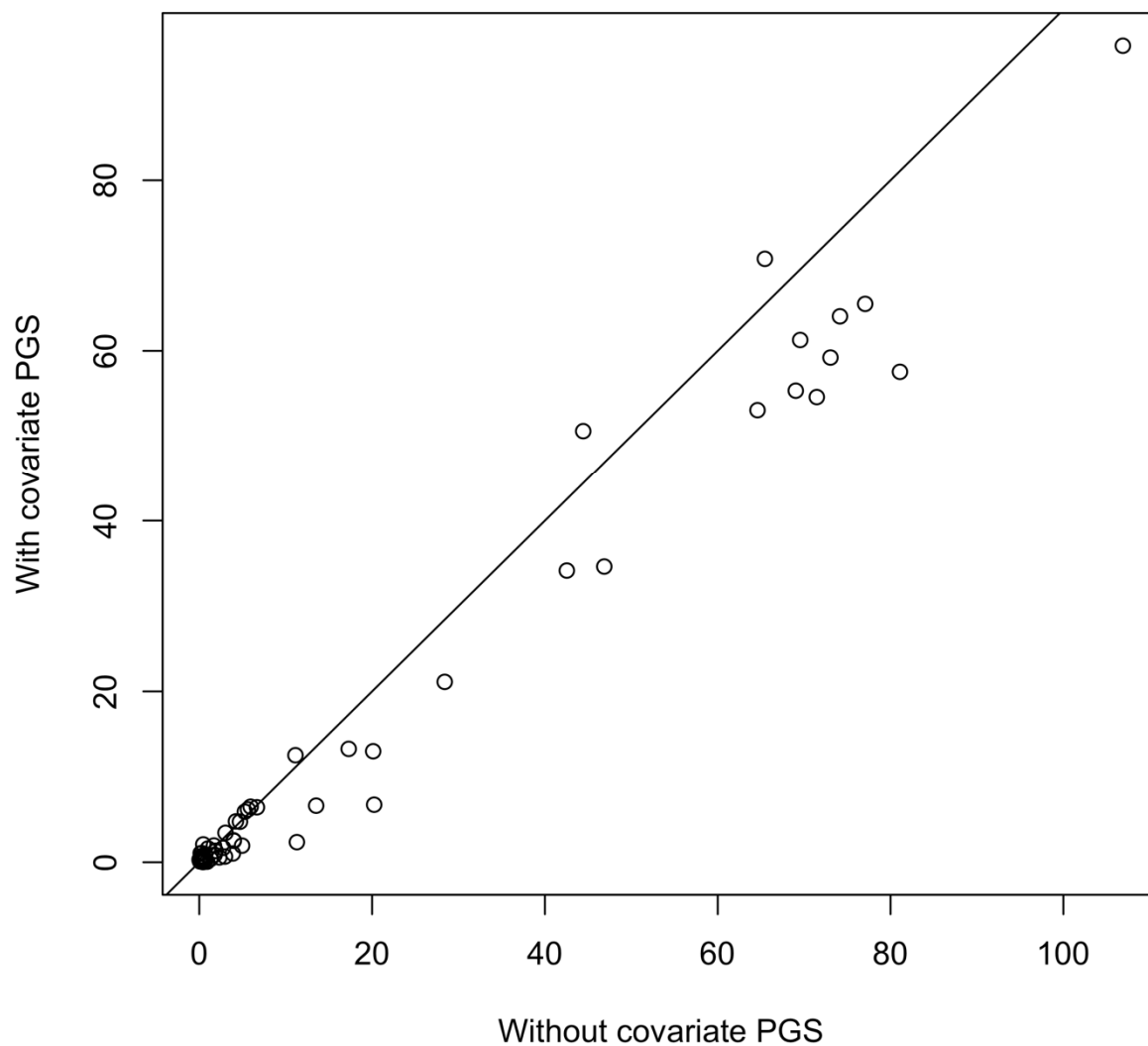
Figure 6. Model R² from different machine learning models across cohorts and ancestries using age and gender as covariates (along with PGS_{BMI} and PCs 1-5). Across all cohorts and ancestries, LASSO with PGS-age and PGS-gender interaction terms had better average 10-fold cross-validation R² than LASSO without interaction terms, while neural networks outperformed LASSO models.



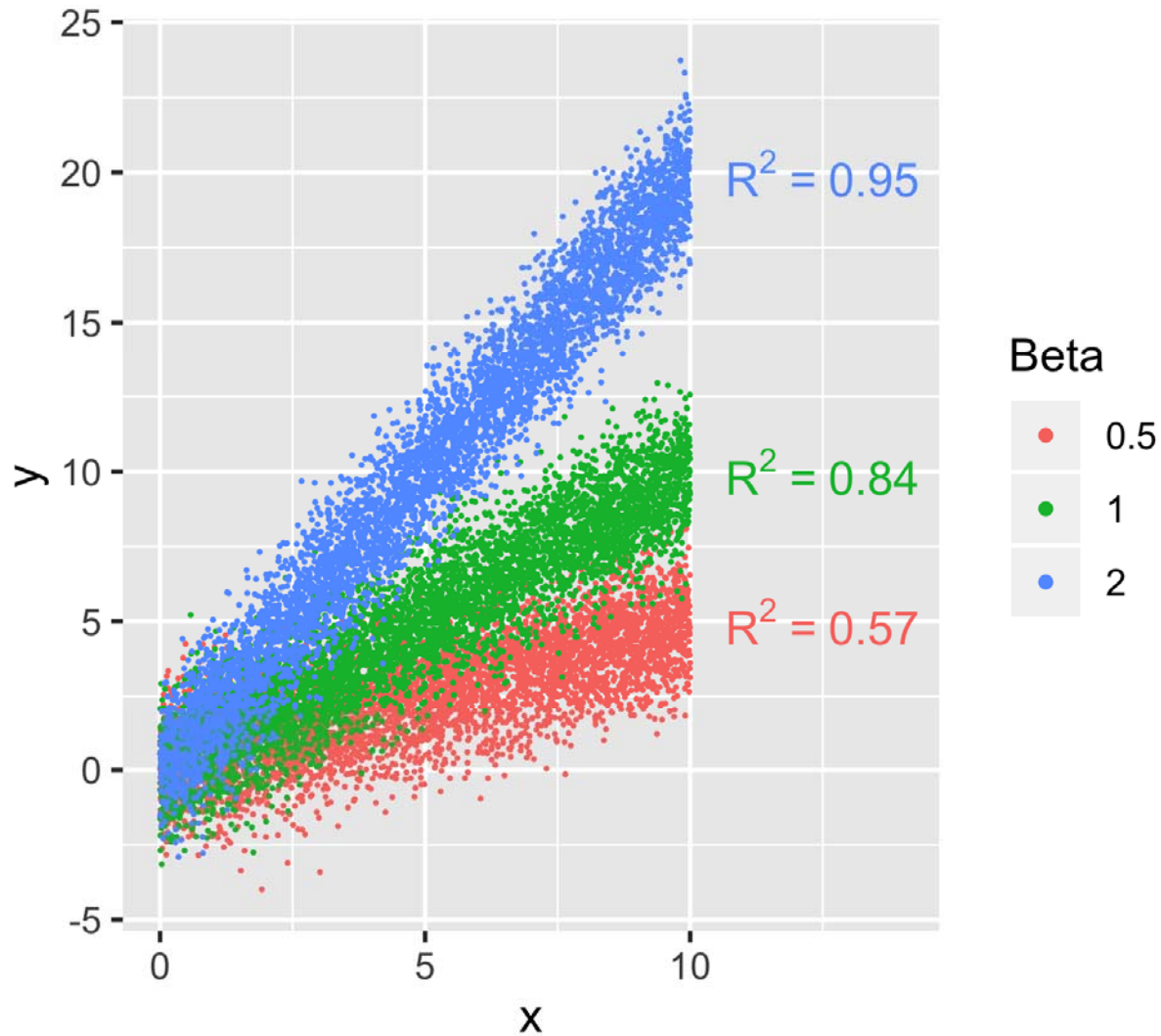
896
897 Figure 7. PGS R² based on three sets of GWAS setups. “Main effects” were from a typical main
898 effect GWAS, “GxAge” effects were from a GWAS with a SNP-age interaction term, and “Age
899 stratified” GWAS had main effects only but were conducted in four age quartiles. PGS R² was
900 evaluated using two models: one with main effects only, and one with an additional PGS*Age
901 interaction term.

902
903
904
905
906
907
908
909
910
911
912
913
914
915
916
917

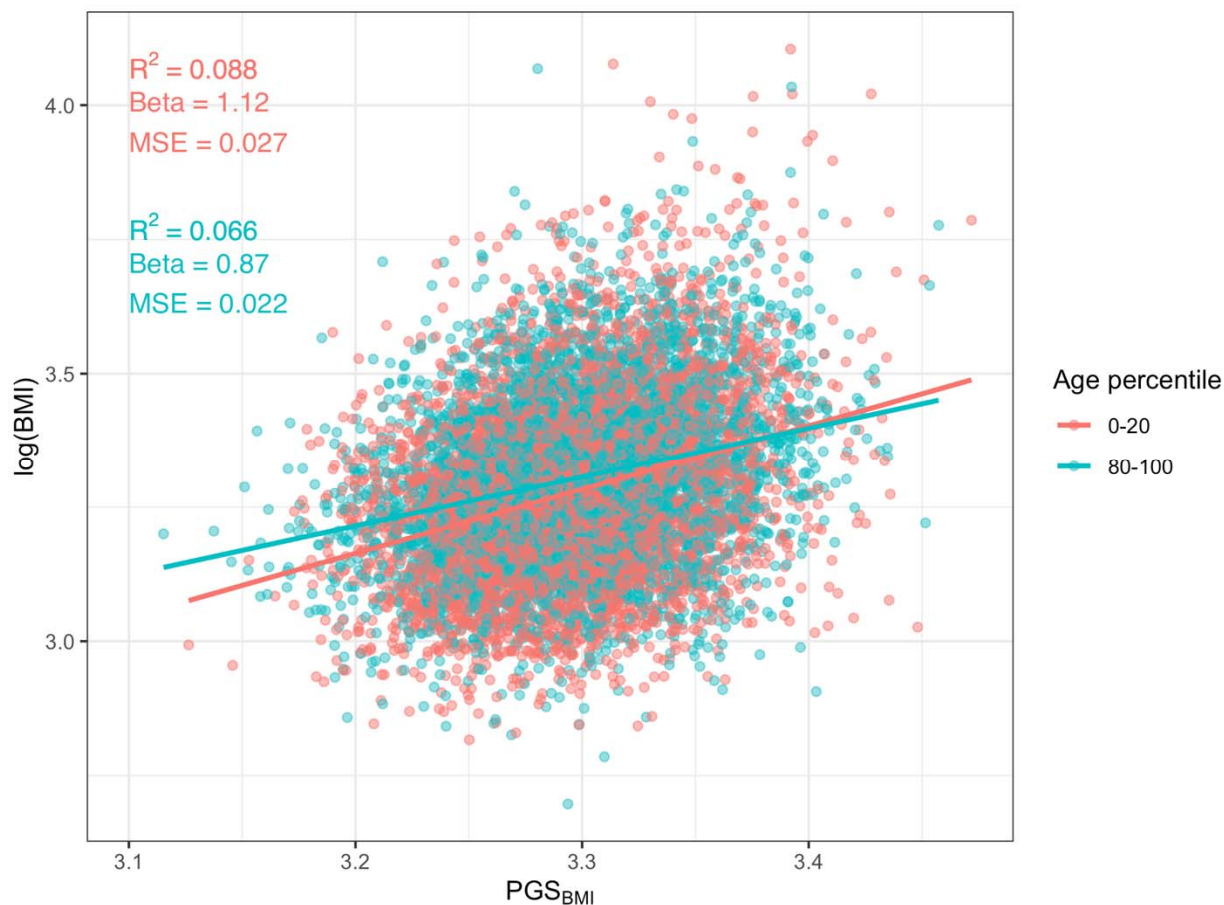
918 Supplemental Figures:



919
920 S Figure 1. PGS-covariate interaction term $-\log_{10}(\text{p-values})$ in UKBB EUR, with and without
921 including the covariate PGS in the model – the mean $-\log_{10}(\text{p})$ is reduced from 18.0899 to
922 14.97072 with their inclusions. Note age and sex PGS were not calculated, and their interaction
923 p-values are excluded from this figure.



924
925 S Figure 2. Three sets of simulated data with varying regression line slopes, showing how model
926 R^2 changes when regression line slope changes, all else being equal. Residuals were sampled
927 from a normal distribution (mean=0, sigma= $\sqrt{\pi/2}$) to give mean squared error=1. 5,000 x-
928 values were sampled for each line, uniformly distributed from 0-10. Despite having the same
929 mean squared error, model R^2 increases as beta increases.
930



931
 932 S Figure 3. Univariable association of PGS_{BMI} and $\log(BMI)$ in European UKBB, separately for
 933 the bottom and top quintiles of age. R^2 is higher in younger individuals, which is partially a
 934 consequence of the larger effect (as shown in S Figure 2), despite the mean squared error
 935 actually being higher.

936
 937 **Table**

Variable type	Covariate	% change in β_{PGS} per covariate unit change	Interaction P	R^2 increase with interaction term	N
Continuous	HDL cholesterol	-15.29	1.71×10^{-96}	0.0012	328719
	Total cholesterol	-12.70	1.64×10^{-71}	0.00082	359221
	IPAQ	-12.50	3.11×10^{-66}	0.001	304951
	Moderate-vigorous PA	-11.41	8.92×10^{-65}	0.001	304951
	Diastolic BP	10.84	6.06×10^{-60}	0.0007	352804
	Townsend Index	6.78	2.86×10^{-58}	0.00089	376283
	Age	-9.02	3.60×10^{-57}	0.00061	376729
	FVC	-9.66	4.69×10^{-56}	0.0008	343467
	Drink frequency/wk	-19.96	2.62×10^{-55}	0.0024	122281
	LDL cholesterol	-9.86	2.63×10^{-51}	0.00058	358556
	N days vigorous PA/wk	-9.37	2.42×10^{-35}	0.0007	299963

	FEV1	-7.38	7.15×10^{-35}	0.0005	343544
	Mean alcohol consumption	-7.38	7.65×10^{-22}	0.00113	126756
	HbA1c	4.63	5.37×10^{-14}	0.0002	358798
	Mean drinks/wk	-7.66	1.01×10^{-13}	0.0008	112204
	Water intake	4.60	2.97×10^{-13}	0.00014	347472
	Processed meat intake	3.70	2.38×10^{-7}	0.0002	376205
	Starch mean	5.51	3.15×10^{-7}	0.00018	128346
	Smoking pack years	4.78	3.68×10^{-7}	0.0002	114135
	Protein mean	4.82	6.52×10^{-7}	0.00018	128181
	Saturated fat mean	4.92	1.23×10^{-6}	0.00017	127899
	Fat mean	4.40	1.64×10^{-5}	0.00013	128092
	Saturated fat grams/wk	2.46	1.79×10^{-5}	4.00E-05	364629
	Retinol mean	3.77	3.54×10^{-4}	9.00E-05	126029
Binary	IPAQ	-12.68	5.30×10^{-62}	0.0009	304951
	Vigorous PA/wk	-20.55	9.07×10^{-54}	0.0009	304951
	Sex	-11.02	1.41×10^{-24}	0.00025	376729
	Diabetes	27.19	1.83×10^{-7}	0.0004	375903

938

939 Table 1. Model descriptive statistics on 28 of 62 covariates, which have significant ($p < .05/62$)
 940 PGS-covariate interaction terms, in UKBB EUR. The third column is the percentage change in
 941 PGS effect per unit change (standard deviations for continuous variables, binary variables
 942 encoded as 0 or 1) in covariate. The fifth column is the increase in model R^2 with a PGS-
 943 covariate interaction term versus a main effects only model. Abbreviations: blood pressure (BP),
 944 physical activity (PA), forced vital capacity (FVC), forced expiratory volume in 1-second
 945 (FEV1), International Physical Activity Questionnaire (IPAQ).